PAPER • **OPEN ACCESS**

Preliminary analysis of an integrated ICE-gasifier plant for power generation from plastic waste material

Journal of Physics: Conference Series **2893** (2024) 012022 doi:10.1088/1742-6596/2893/1/012022

Preliminary analysis of an integrated ICE-gasifier plant for power generation from plastic waste material

N Grilli[1], M Ciampolini[1], L Bosi[1], L Romani[1*], and G Ferrara[1]

[1] Department of Industrial Engineering, Università degli Studi di Firenze, via di Santa Marta 3, 50139 Firenze, Italy

* Contact Author: luca.romani@unifi.it

Abstract. The escalating global production of plastic waste is a challenge that must be rapidly addressed, but it also conceals opportunities. Currently, only a minor portion of the worldwide plastic waste is recycled, with the remainder destined for either incineration or landfill. In this context, gasification emerges as a sustainable alternative to conventional waste management methods, offering a substantial reduction in pollutant emissions. Dioxins and furans emissions, in fact, are drastically reduced when compared to incineration. Additionally, in contrast to landfill disposal, gasification allows for the recovery of chemical energy contained in plastic that would otherwise be wasted. The study of plastic gasification is gaining attention and several studies demonstrated feasibility and effectiveness, despite it is not as established as biomass gasification. The present paper aims at taking a step forward by conceptualizing an integrated gasifier-internal combustion engine power plant, operating in a closed-loop system. This layout offers potential benefits from both energetic and environmental points of view, respectively related to the recovery of engine waste gas and CO_2 emission reduction. The proposed plant is based on the steam/CO_2 gasification technique, which allows the complete conversion of input CO_2 into syngas under certain thermochemical conditions. This feature enables the operation of engine and gasifier in a closed-loop system, directly exploiting the exhaust gas to perform plastic gasification. A thermodynamic feasibility study is performed, accounting for the efficiency of the main components, the heat fluxes and the heat absorbed by the endothermic reactions inside the gasifier. The setup of the proposed power plant shows an energy conversion efficiency up to 18% in a pure electric generation scenario and up to 56% in a cogeneration scenario.

1. Introduction

With global plastic waste production now estimated at around 396 Mt per year [1], waste management is one of the biggest challenges for humankind in the near future. In fact, global plastic waste production has extraordinarily increased compared to the 2 Mt value of 1950 [2], and it is predicted to pass 600 Mt in 2023 [3]. Plastic waste is composed of several different materials, including PET (polyethylene terephthalate), HDPE (high-density polyethylene), LDPE (low-density polyethylene), DP (polypropylene), PS (polystyrene), PVC (polyvinyl chloride) and rubber. The majority of this waste ends up either incinerated or in landfills, leading to environmental pollution or loss of energy resources [4]. Incineration is by far the greatest CO_2 emission source of plastic end-of-life management options. Plastic landfills cause considerably lower emissions than incineration; however, waste plastic storage in mixed landfills causes severe ground and groundwater pollution due to the leaching of toxic additives caused by favourable reducing conditions [5]. In 2015, the global plastic recycling rate was about 19.5%, compared to 25.5% incineration and 55% landfill storage [5]. In Europe, the situation seems to be less severe, accounting for a total plastic waste production of 29.5 Mt in 2020, distributed in 35% recycling, 42% incineration and 23% landfill storage [6]. However, despite the lower contribution in absolute terms, the European data are also concerning, dealing with the Country with the highest plastic recycling rate. Thus, innovative solutions are essential to address this escalating problem and one promising approach is gasification. Gasification is an endothermic process that converts a solid fuel into a gaseous fuel known as synthesis gas, or syngas, whose properties depend on the solid fuel employed and the gasification agents. Gasification offers several advantages over other waste management techniques: it substantially reduces the emission of hazardous pollutants such as dioxins and furans, commonly produced during incineration, and allows for the recovery of chemical energy contained in plastic waste, which would otherwise be lost in landfills. Furthermore, the residual volume can be drastically reduced by means of this

technology, allowing for a reduced impact of plastic waste disposal on landfill soil occupation. Despite these benefits, even gasification typically causes CO_2 emission since the endothermic process requires a high amount of external heat at high temperature, which is difficult to supply via renewables [5]. Thus, it could be useful to include gasification plants into integrated systems of energy generation capable of further reducing the total CO_2 emission balance. The main gasification processes available for plastic gasification are air gasification, steam gasification, CO_2 gasification and mixed CO_2/steam gasification [7, 8]. A smart technique seems to be the combination of a gasifier with an internal combustion engine (ICE), which presents high-temperature gas composed of CO_2 and H_2O at the exhaust. The exhausts can thus be supplied at the inlet of a gasifier based on CO_2/steam gasification, and the produced syngas can be used in closed-loop to fuel the ICE. The present paper will thus discuss the feasibility of such integrated system from a thermodynamic point of view, focusing on both electric and thermal generation capabilities. This innovative concept, which seems to be missing in the literature to the best of the Authors' knowledge, may result useful in those industrial processes requiring high-temperature heat (e.g., annealing and normalization in the steelwork industry, ovens in the ceramic industry, rotating ovens in the concrete production, etc.) or low-temperature heat (e.g., drying process in the textile and paper industry, etc.).

2. Materials and methods

In the present Section, the entire methodology adopted to study the thermodynamic feasibility of a closed-loop engine/gasifier power plant is assessed. In the following Chapters, the chemical reactions occurring in a high-temperature CO_2/steam gasifier are presented at first (Section 2.1), followed by the characteristics and components of the proposed plant layout (Section 2.2). Finally, Section 2.3 will present the main balance equations for species, thermal and mass equilibrium, together with the hypothesis concerning the operating temperature in the main plant positions.

2.1 Chemical reactions in the gasifier

Studies on the gasification of a typical mix of plastic waste have shown that CO_2 and steam can be effectively used as gasification agents [8]. This process produces syngas with a high hydrogen content and it can theoretically achieve the complete conversion of the introduced CO_2. This feature is a crucial characteristic to prevent CO_2 accumulation in closed-loop systems. From an environmental point of view, a closed-loop system could be highly beneficial since it allows us to exploit waste products by means of an ICE for power generation, curtaining the net CO_2 emissions in the atmosphere.

To correctly convert the whole CO_2 amount in the gasifier, it is required to keep the gasifier temperature above 700°C; by doing so, the Boudouard reaction is strongly shifted to the right (Equation 1).

$$C + CO_2 \leftrightarrow 2CO \quad (1)$$

For the complete conversion of CO_2, it is advisable to operate even at higher temperatures, i.e., around 900°C. Since the reactions occurring in the gasifier are predominantly endothermic, external heating is required in this configuration.

Table 1. Chemical reactions in CO_2/steam gasification. Data from [8].

No.	Reaction	Heat [kJ/mol]	No.	Reaction	Heat [kJ/mol]
1	$C + ½O_2 \leftrightarrow CO$	−112	7	$C + CO_2 \leftrightarrow 2CO$	171
2	$CO + ½O_2 \leftrightarrow CO_2$	−283	8	$CnHm + nCO_2 \leftrightarrow 2nCO + ½mH_2$	endoth.
3	$H_2 + ½O_2 \leftrightarrow H_2O$	−248	9	$C + 2H_2 \leftrightarrow CH_4$	−74.8
4	$C + H_2O \leftrightarrow CO + H_2$	136	10	$CO + 3H_2 \leftrightarrow CH_4 + H_2O$	−225
5	$CO + H_2O \leftrightarrow CO_2 + H_2$	−35	11	$CO_2 + 4H_2 \leftrightarrow CH_4 + 2H_2O$	−190
6	$CH_4 + H_2O \leftrightarrow CO + 3H_2$	206			

Table 1 reports the main chemical reactions occurring in the gasifier [8]. The most significant reactions investigated in [8], at a temperature of about 700°C, are i) dry reforming with light hydrocarbons (no. 8 in

Table 1), ii) water-gas shift reaction (no. 5), and iii) Boudouard reaction (no. 7). According to Kannan et al. [8], gasification processes at a temperature above 600°C are not limited by chemical kinetics and can be studied using equilibrium models. The species considered at equilibrium are C, CO, CO_2, O_2, N_2, H_2, H_2O, and CH_4, while heavy hydrocarbons are not thermodynamically stable under gasification conditions.

2.2 Layout of the proposed plant

The proposed closed-circuit plant layout, mainly composed of a spark-ignition ICE for power generation use, CO_2/steam gasifier, oxygen separator, methane/syngas burner, ash and tar filters, and several heat exchangers is depicted in Figure 1.

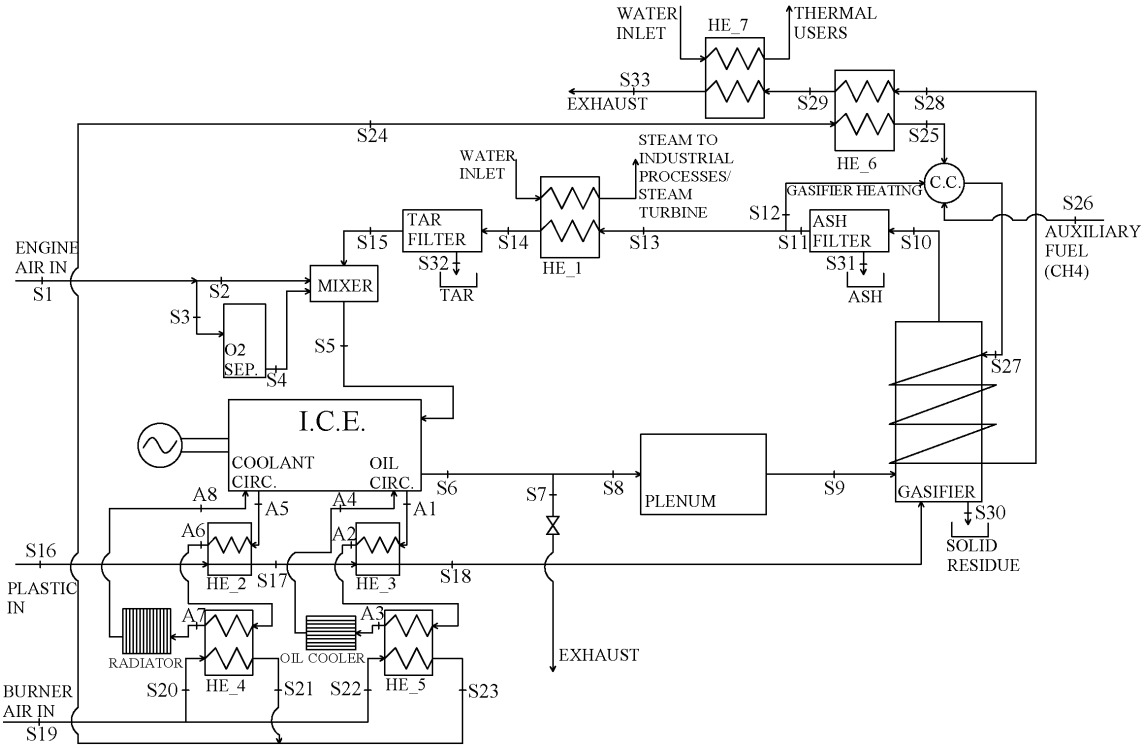

Figure 1. Schematic draw of the proposed engine/gasifier closed-loop power plant.

The oxygen separator (S3 to S4), removing a certain amount of nitrogen from fresh air, is crucial in the closed-loop layout, since it prevents uncontrolled nitrogen accumulation in the plant. In fact, without that component, new nitrogen would be added cycle-by-cycle together with the oxygen required for the combustion in the engine. In steady-state operation, the mass flow passing through S2 (air inlet to mixer) and S4 (oxygen inlet to mixture) has to be regulated so that the total amount of nitrogen that enters the circuit is the same of that leaving the circuit in S12 (burner syngas inlet), keeping the total inert content constant during operation. The amount of nitrogen in the closed-loop circuit can be adjusted according to the desired operating conditions; in particular, it was assumed to match the imposed maximum engine exhaust gas temperature in S6. Since engine exhaust gas is directly used as gasification agent, combustion must be stoichiometric not to present oxygen content at the exhaust. Therefore, in order to control the outlet temperature at the exhaust it is required to change the total amount of inert gases inside the engine. The plant is conceptualized to operate with a spark-ignition four-stroke medium-size engine for power generation, with a rated output power of 100 kW.

In the proposed plant, fresh air enters S1 and it is split into two different pipes: a portion (S2) is directly driven into an air/oxygen/syngas mixer in order to prepare the premixed fuel mixture sent to the engine (S5); the other part (S3) is sent into an oxygen separator capable of extracting oxygen from the inlet air. The pure oxygen is then driven into the mixer (S4).

The engine burns the syngas/oxygen/nitrogen mixture producing hot exhaust gas (S6) composed of CO_2, H_2O vapour and N_2. Section S7 is a normally closed branch of the circuit and is meant to be used only when there

is the necessity to renew the closed-circuit gas (in case of accidental nitrogen accumulation). The exhaust gas is sent in a plenum to stabilize pressure and flow rate.
The exhaust gas then enters the gasifier (S9), together with pre-heated plastic waste (S18). In fact, the plastic mix entering the system (S16) passes through two heat exchangers (HE2 and HE3), recovering heat from engine coolant and oil circuits. The gasifier is kept at a constant temperature of 900°C by means of an external heating circuit (S27 to S28). The outputs of the gasifier are the syngas (S10) and the solid residue (S30).
A filter removes the ash content from the syngas (S31); then, the latter is split into two pipes: one returns towards the engine (S13), while the other is sent to the burner to sustain the gasifier external heating (S12). The mass flow through S13 is regulated to obtain the 100kW power output at the engine.
In order to achieve the desired engine inlet temperature in S5, the syngas, void of TAR contents by means of a dedicated filter (S15), is cooled before mixing with fresh air and oxygen in a heat exchanger (HE1). The heat recovered by syngas is used to produce steam, which can either be employed directly as process steam (cogeneration scenario) or driven to a steam microturbine (pure power generation scenario) to increase the net electric energy production. It is worth noting that since TAR condensation depends on the gas temperature, a minimum temperature of 150°C was imposed in S5 in order to prevent both high TAR condensation and auto-ignition phenomena in the ICE.
Concerning the gasifier heating circuit, air passing through S19 is split into two equal pipes (S20 and S22) and sent to two heat exchangers (HE4 and HE5) in order to pre-heat air by means of engine coolant and oil heat. The air is then conveyed in a single pipe again (S24) and driven to a heat exchanger (HE6), adopting the residual heat of the gasifier heating circuit (S28) to preheat the fresh air. The preheating temperature in S25 is a key parameter and it will be subjected to sensitivity analysis. The preheated air (S25), hot excess syngas (S12), and auxiliary methane (S26) are driven into the burner, which output gas (S27) is conveyed into the gasifier heating liner to sustain the endothermic reactions. The gas flowing out of the liner (S28) and driven to HE6 is assumed to be further cooled down up to 50°C in another heat exchanger (HE7) in order to produce hot industrial water or for thermal users in general.

2.3 Modelling methodology

The commercial software EES (Engineering Equation Solver) was chosen to model the thermodynamic system due to its robust capability to solve complex non-linear equations and its extensive library of thermophysical properties. This combination ensures accurate and efficient analysis of the system's behaviour.
According to [9], the plastic mix fed to a gasifier is composed of LDPE, HDPE, PS, PET, PP, PVC, and other minor species. In the present paper, the latter was assumed to be equally divided into rubber, PMMA, and PA-6. Furthermore, in order to avoid the formation of strong acids (e.g., hydrochloric acid) caused by chlorine, it was assumed that PVC is totally removed from the plastic mix before entering the gasifier. This assumption is required to preserve the plant components and avoid the requirement for an additional filtration system. The calorific value of each species was considered when calculating the overall calorific value of the incoming mass of plastics. It is worth noting that the calorific values presented in the referenced sources [9] and [10] show moderate discrepancies; thus, an average value was used. The assumed plastic waste composition, along with the heating value of each component, is summarized in Table 2.

Table 2. Assumptions on plastic material low heating value.

Material	Mass fraction	LHV [MJ/kg]	Material	Mass fraction	LHV [MJ/kg]
Rubber	1.7	42.4	PS	4.9	39.6
PA-6	1.7	30.2	PP	7.5	43.5
PMMA	1.7	25.0	HDPE	58.7	34.1
PET	6.0	22.2	LDPE	17.8	38.9

Considering that composition, the resulting low heating value (LHV) of the plastic mix equals to 35.13 MJ/kg.
All heat exchange equations are based on the $\dot{m} \cdot cp \cdot \Delta T$ formulation. Specific heat is computed as the integral average value in the $(T - T_{REF})$ range, in which T_{REF} is the reference temperature, assumed equal to 15°C.
It was assumed that the entire amount of exhaust gas from the engine is used for syngas production. Dealing with a closed loop system, it was also assumed that the amount of syngas (produced by the gasifier) not required

to fuel the engine is used to provide heat to the endothermic reactions of the gasifier. Considering i) the gasification reactions presented in Table 1, ii) the composition of the gas entering and exiting the gasifier, iii) the cold gas efficiency (CGE) of the process, iv) the calorific value and molar composition of the plastic mix (Table 2), the balance equations for the gasifier can be written:

$$m_{18} \cdot LHV_{PL} \cdot CGE = m_{10} \cdot LHV_{SYN} \quad (2)$$

$$LHV_{SYN} = LHV_{H2} \cdot MFS_{H2} + LHV_{CO} \cdot MFS_{CO} + LHV_{CH4} \cdot MFS_{CH4} \quad (3)$$

$$N_{CO2} = R_{CO2/C} \cdot N_C \quad (4)$$

$$m_{27} \cdot cp_{27/28} \cdot (T_{27} - T_{28}) \cdot \eta_{COIL} = QR_{16} \cdot m_{16} - m_9 \cdot cp_{10EXH} \cdot (T_9 - T_{10}) + m_{16} \cdot cpm_{16} \cdot (T_{10} - T_{18}) \quad (5)$$

$$m_9 + m_{18} = m_{10} + m_{30} + m_{10ASH} + m_{10TAR} \quad (6)$$

Equation 2 is an energy balance at the gasifier, where on the left-hand side of the equation m_{18} is the mass flow of the inlet plastics, LHV_{PL} the plastics mean heating value, GCE the cold gas efficiency (defined by [8]); on the right-hand side, m_{10} is the mass flow rate of the produced syngas and LHV_{SYN} is the synthesis gas heating value, expressed in Equation 3. The syngas LHV depends on its composition (MFS_{H2}, MFS_{CO}, and MFS_{CH4} represent respectively the mass fraction of H_2, CO, and CH_4 in the syngas). It is worth noting that the syngas composition depends on the gasification agent composition (engine exhaust gas), which in turn depends on the syngas composition itself. For this reason, the solution is iterative. Furthermore, the actual mass fraction in the plant depends on the amount of N_2 in the circuit, which has a "dilution" effect, lowering the LHV_{SYN} value. Equation 4 is a chemical relationship between the number of moles of CO_2 that enters the gasifier through the exhaust gas and the number of carbon moles that enter through the plastic mix. The ratio between these two values ($R_{CO2/C}$) is a crucial parameter (in addition to temperature, which must be kept higher than 700 °C) in determining the composition of the syngas. This value was chosen the highest possible still guarantying a complete CO_2 conversion, i.e., 0.454. The latter assumption agrees with the data presented by Kannan et al. [8] and must be insured in order to run the closed-loop system. The amount of incoming plastic is evaluated based on the gasification conditions, the moles of CO_2 in the gas entering the gasifier, and the moles of carbon in the plastic itself.
Equation 5 is the heat balance between the heat transferred by the gasifier heating system (left-hand side) and the heat absorbed by the chemical reactions in the gasifier. In particular, on the right-hand side, it can be found respectively i) the heat absorbed by the endothermic gasification reactions, ii) the heat required to raise the exhaust gas temperature up to the gasifier temperature, and iii) the heat necessary to raise the plastic waste temperature up to the gasifier temperature. Finally, Equation 6 is a mass balance of the gasifier that allows us the computation of the solid residual amount (m_{30}).
The maximum operating temperature of the gasifier heating liner was assumed to be equal to 1150°C (S27) based on the technological limits of materials. The assumed heat exchange efficiency is 95%.
The internal combustion engine size is fixed to 100 kW electric net power output. Engine efficiency, energy split, and operating temperatures are assumed based on best available technologies concerning steady-state spark-ignition engines. The assigned values are resumed in Table 3.

Table 3. Assumptions on engine heat distribution and operating temperatures.

Energy portion	Sym.	Value	SI	Temperature	Sym.	Value	SI
Engine efficiency	η_{ICE}	35	%	Oil in (A4)	$T_{oil,in}$	75	[°C]
Energy to exhaust	L_{exh}	35	%	Oil out (A1)	$T_{oil,out}$	85	[°C]
Energy to oil circuit	L_{oil}	12.5	%	Water in (A8)	$T_{w,in}$	75	[°C]
Energy to water circuit	L_w	12.5	%	Water out (A5)	$T_{w,out}$	85	[°C]
Energy to radiation	L_{rad}	5	%	Fuel inlet (S5)	T_{fuel}	150	[°C]

Engine exhaust temperature was considered to be equal to 800°C in normal conditions. Thus, a sensitivity analysis was also carried out by setting this value between 750°C and 900°C (step of 50°C) in order to understand the effect of this parameter on system performance in power generation and cogeneration scenarios.

Concerning the ICE, intended as an electric generation system, the following balance equations can be written:

$$\eta_{ICE} \cdot (m_{15} \cdot LHV_{SYN}) = W_{ICE} \quad (7)$$

$$m_5 \cdot cp_5 \cdot (T_5 - T_{REF}) + L_{EXH} \cdot W_{ICE} / \eta_{ICE} = m_6 \cdot cp_6 \cdot (T_6 - T_{REF}) \quad (8)$$

Equation 7 is the energy balance at the ICE, which allows us to compute the syngas mass flow (m_{15}) given the engine efficiency (η_{ICE}), the rated output power (W_{ICE}), and the expression for the syngas lower heating value (Equation 3). Equation 8 is the energy balance for the engine exhaust gas. On the left-hand side, there is the sensible heat of the entering mass flow (m_5) and the heat transferred to the exhaust gas causing the rise of the temperature; on the right-hand side instead, the sensible heat of the gas leaving the ICE (m_6) can be found. It is worth noting that the heat transferred to the gas only affects the mass entering the engine since the intake and exhaust temperature are both fixed by technological limits. The mass entering the engine (m_5) is conceptually composed of a portion of syngas, giving the necessary heat, a portion of oxygen necessary to the combustion of the syngas, and a portion of inert nitrogen. The percentage of nitrogen circulating in the plant is thus evaluated on the exhaust temperature basis, and can be practically regulated by acting on the air/pure oxygen proportions in sections S2 and S4 of the plant.
Thermal losses in piping from the engine outlet (S6) to gasifier inlet (S9) are estimated in a 30°C temperature drop. The temperature drop occurring in hot syngas piping, instead, is assumed to be 20°C in correspondence of the ash filter (S10 to S11) and 15°C of the tar filter (S14 to S15).
The efficiency of heat exchangers was estimated according to the typology: i) 94% for air/air exchangers (η_{AA}), ii) 96% for air/liquid exchangers (η_{AL}), and iii) 98% for liquid/liquid exchangers (η_{LL}).
The preheating temperatures in the heat exchangers are set by defining a minimum pinch-point value on one side, and the resulting temperature difference on the other side is computed using the specific heat and mass flows. The a-priori-defined temperatures are: i) 55°C, first plastic preheat temperature (S17), ii) 80°C, second plastic preheat temperature (S18), iii) 80°C, first air preheat temperature (S21 and S23), iv) 800°C, second air preheat temperature (S25).

3. Results

The present Section, in which the results of the present activity are depicted, is divided into two parts. At first (Section 3.1), the operating conditions (temperature, mass flow, and species of the fluid medium) in all the sections of the proposed plant are shown, together with the resulting efficiency values (in terms of both electric generation and cogeneration). Results will account for a single reference value of temperature at the engine exhaust and burner air inlet. In the second Chapter (3.2), a sensitivity analysis concerning the effects of the variation of the two critical temperatures (engine exhaust and burner air inlet) on the efficiency of the power plant is shown, in order to understand the potential benefits of a proper plant setup.

3.1 Operating values at imposed conditions

The operating temperature, mass flow, and species composition of the working fluid in the 33 main sections of the power plant are shown in Table 4. It is worth pointing out that the present results refer to the base plant setup, in which both engine outlet temperature (S6) and air pre-heat temperature (S25, burner inlet) are set at 800°C. This assumption well agrees with the hypothesis of adopting high-alloy steel in these zones. Table 5 instead shows temperature and mass flow values in the engine cooling circuits (coolant and oil, A1 to A8). Furthermore, the main power flows to/from the system are summarized in Table 6.
The efficiency of the proposed power plant was evaluated in two different ways, concerning a pure electric generation scenario (η_{PP}) and a cogeneration scenario (η_{COG}) respectively. For both the two scenarios, efficiency has been evaluated by including the plastic mix heating value (energy point of view, left side of Table 7) and neglecting it (practical point of view, considering the plastic material a “costless” system input, right side of Table 7).
It is worth noting that η_{PP} is evaluated in an “electric-target” plant configuration, in which the steam produced in the heat exchanger HE1 is employed in a hypothetical steam microturbine (assuming for the latter a 23% efficiency) and the heat transferred in the exchanger HE7 is not considered a useful system output. Instead, η_{COG} is evaluated in the cogeneration scenario, in which the heat of both the high-temperature and low temperature exchangers (HE1 and HE7 respectively) is employed for industrial thermal processes and thus considered a useful system outout.

Table 4. Temperature, mass flow, and composition in the sections of the power plant.

n	T [°C]	ṁ [kg/h]	Composition [% mass]						
			H2O	CO2	N2	CH4	H2	CO	O2
S1	20	266.9	0	0	76.46	0	0	0	23.54
S2	20	221.8	0	0	76.46	0	0	0	23.54
S3	20	45.1	0	0	76.46	0	0	0	23.54
S4	20	10.6	0	0	0	0	0	0	100
S5	150	470.2	0.47	0	73.78	0.42	0.66	11.3	13.37
S6	800	470.2	7.32	18.9	73.78	0	0	0	0
S7	800	0	7.32	18.9	73.78	0	0	0	0
S8	800	470.2	7.32	18.9	73.78	0	0	0	0
S9	770	470.2	7.32	18.9	73.78	0	0	0	0
S10	900	470.8	0.94	0	74.58	0.83	1.3	22.35	0
S11	880	468.9	0.94	0	74.58	0.83	1.3	22.35	0
S12	880	229.2	0.94	0	74.58	0.83	1.3	22.35	0
S13	880	239.7	0.94	0	74.58	0.83	1.3	22.35	0
S14	276.3	239.7	0.94	0	74.58	0.83	1.3	22.35	0
S15	261.3	237.8	0.94	0	74.58	0.83	1.3	22.35	0
S16	20	63.7	/	/	/	/	/	/	/
S17	55	63.7	/	/	/	/	/	/	/
S18	80	63.7	/	/	/	/	/	/	/
S19	20	2950.2	0	0	76.46	0	0	0	23.54
S20	20	1475.1	0	0	76.46	0	0	0	23.54
S21	80	1475.1	0	0	76.46	0	0	0	23.54
S22	20	1475.1	0	0	76.46	0	0	0	23.54
S23	80	1475.1	0	0	76.46	0	0	0	23.54
S24	80	2950.2	0	0	76.46	0	0	0	23.54
S25	800	2950.2	0	0	76.46	0	0	0	23.54
S26	20	7.56	0	0	0	100	0	0	0
S27	1150	3185.3	1.57	3.32	76.14	0	0	0	18.97
S28	920	3185.3	1.57	3.32	76.14	0	0	0	18.97
S29	243.8	3185.3	1.57	3.32	76.14	0	0	0	18.97
S30	900	63	/	/	/	/	/	/	/
S31	900	1.89	/	/	/	/	/	/	/
S32	261.3	1.95	/	/	/	/	/	/	/
S33	50	3185.3	1.57	3.32	76.14	0	0	0	18.97

Table 5. Temperature and mass flow in the sections of the engine cooling circuit.

n	T [°C]	ṁ [kg/h]	Fluid	n	T [°C]	ṁ [kg/h]	Fluid
A1	85.0	6123.6	Oil	A5	85.0	3063.6	Coolant
A2	84.7	6123.6	Oil	A6	84.7	3063.6	Coolant
A3	77.2	6123.6	Oil	A7	77.5	3063.6	Coolant
A4	75.0	6123.6	Oil	A8	75.0	3063.6	Coolant

Table 6. Power input/output of the proposed plant in the baseline configuration.

Zone	Description	W [kW]	Zone	Description	W [kW]
S16	plastic inlet	621.3	S26	methane inlet	105.0
HE1	high-temp. heat	51.6	HE7	low-temp. heat	169.9

Table 7. Efficiency indictors of the proposed plant in the baseline configuration.

Sym.	Description	η [-]	Sym.	Description	η [-]
η_{PP}	electric, 1st principle	0.154	η_{PP}	electric, w/o plastic	1.065
η_{COG}	cogeneration, 1st principle	0.443	η_{COG}	cogeneration, w/o plastic	3.062

3.2 Sensitivity analysis

Exhaust gas temperature (T_6) influences both the closed-loop balances and the gasifier heating circuit. In detail, it strongly influences the mass flowing through the engine, which has to be more diluted by nitrogen content as the outlet temperature is lowered. This feature affects the methane mass flow required at the burner and the oxygen mass flow at the separator, respectively depicted in Figure 2A and Figure 2B.

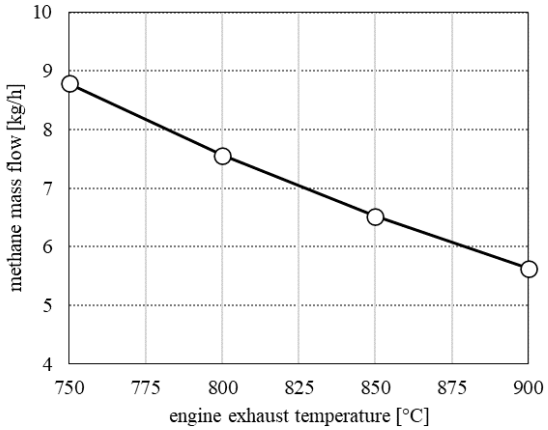

Figure 2A. Effect of engine outlet temperature (S6) on methane mass flow in the burner (S26).

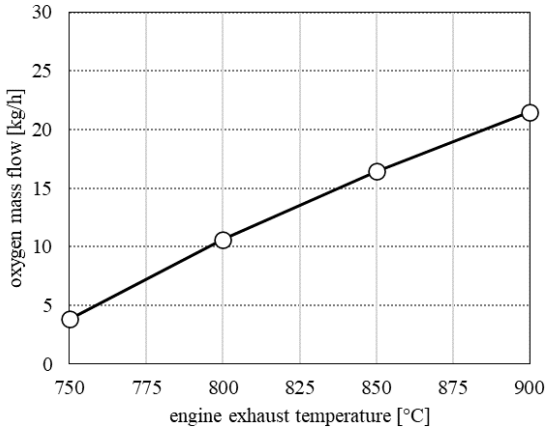

Figure 2B. Effect of engine outlet temperature (S6) on oxygen mass flow below separator (S4).

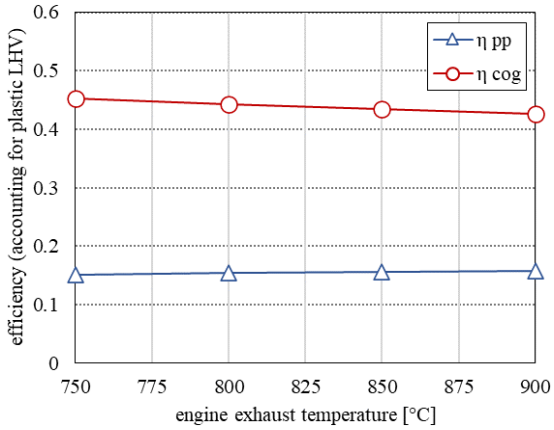

Figure 3A. Effect of engine outlet temperature (S6) on η_{pp} and η_{cog} accounting for plastic mix LHV.

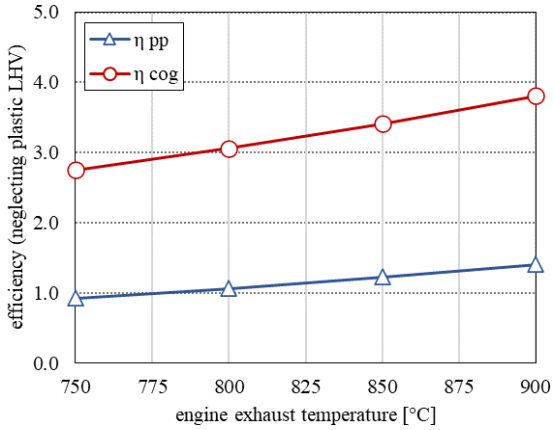

Figure 3B. Effect of engine outlet temperature (S6) on η_{pp} and η_{cog} neglecting plastic mix LHV.

Concerning the plant efficiency, a rise in exhaust temperature makes the efficiencies rise (Figure 3A and 3B), except for the cogeneration efficiency accounting for plastic LHV, which slightly decreases. This behaviour is due to the fact that a higher exhaust temperature modifies the mass flow in S12, which decreases due to the lower nitrogen content. This alters the balances at the burner and at the HE6 exchanger, resulting in a lower temperature T_{29} and, thus, in a reduction of the available heat in HE7. The increase in pure power production efficiency, instead, means that the heat provided by the auxiliary methane decreases more than the energy production at the steam microturbine. The reduction of turbine electric production, related to the reduction of heat available at HE1, is due to the reduction of mass flowing through the heat exchanger itself.
Even the air preheat temperature (T_{25}) shows a marked influence on system balances. In particular, the gasifier heating circuit is affected (Figure 4B), whereas the closed-loop ICE-gasifier is not altered. A greater energy recovery from the burner exhaust gas allows us to reduce the auxiliary fuel to be burned into the burner to obtain the desired temperature. It is worth noting that with the highest energy recovery scenario, the auxiliary methane mass flow drops to zero. In such operating condition, the system can sustain itself with no need for external fuels (Figure 4A).

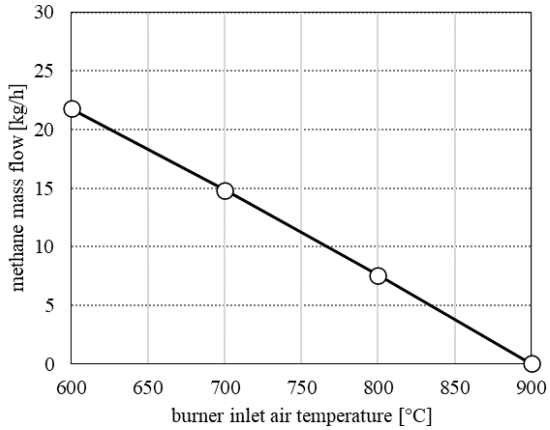

Figure 4A. Effect of burner air temperature (S25) on methane mass flow in the burner (S26).

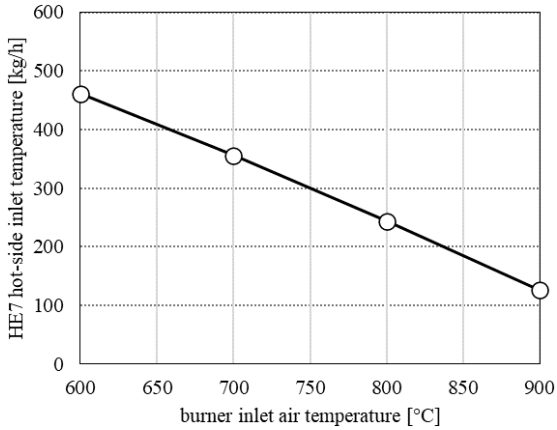

Figure 4B. Effect of burner air temperature (S25) on HE7 inlet temperature, hot-side (S29).

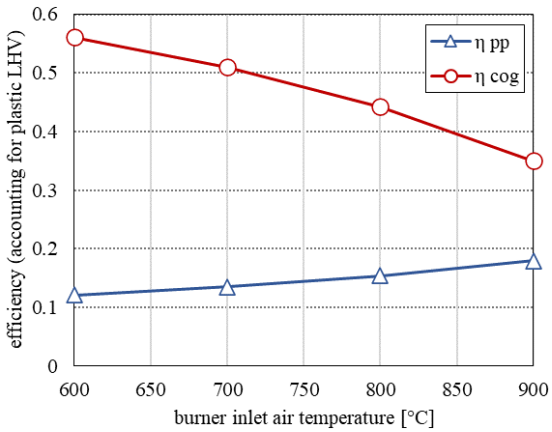

Figure 5A. Effect of burner air temperature (S25) on η_{pp} and η_{cog} accounting for plastic mix LHV.

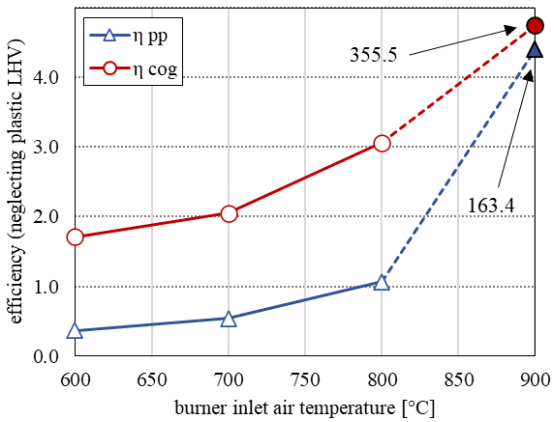

Figure 5B. Effect of burner air temperature (S25) on η_{pp} and η_{cog} neglecting plastic mix LHV.

Looking at the efficiencies (accounting for plastic LHV) it can be observed that while the electric production efficiency rises, the cogeneration efficiency lowers (Figure 5A). This behaviour is due to the greater energy recovery that leads to a lower temperature available for cogeneration at the exchanger HE7. Since the methane combustion is more efficient than energy production through plastic gasification, the efficiency decreases by lowering the mass of burnt methane. It is worth noting that this feature must not be seen as a negative effect, since the main goal of the proposed plant is recovering energy from plastics, while methane utilization for heat

generation is not a matter of interest. If the LHV of plastics is not included in the computation of the efficiency (Figure 7B) instead both the pure power generation and cogeneration present a positive trend by increasing the burner air inlet temperature, showing extremely high values in correspondence of an almost null methane consumption in the burner.

4. Discussion

The engine exhaust temperature was found to be significantly influent on the plant thermodynamic balances. In particular, a higher temperature allows us for an engine size reduction, since the mass flow elaborated by the engine is considerably lower. This is related to the reduced nitrogen content, also influencing the sizing of all other plant components. Furthermore, the auxiliary methane requirement diminishes by increasing the engine outlet temperature, since a minor amount of heat is required to raise the temperature of the exhaust gas up to the gasifier operating temperature (both due to the higher temperature itself and to the reduced mass flow). On the other hand, the mass flow required at the oxygen separator considerably increases by raising the engine exhaust temperature and this may lead to additional plant costs and size. Finally, technical/economic considerations should be made about the materials required to withstand a higher exhaust temperature (e.g., a steel engine piston may be required).

In a cogeneration scenario, attention must be paid to the gas temperature leaving the heat exchanger (HE1). In fact, in the exchanger a condensation of TAR may occur in case of a too low syngas outlet temperature. An experimental evaluation of the relationship between the outlet temperature and the maintenance/cleaning interval of the heat exchanger appears to be fundamental in order to choose the best compromise in terms of cost effectiveness.

A crucial feature for the correct functioning of the plant relates to the CO_2 conversion in the gasifier. In fact, a non-complete conversion would result in CO_2 accumulation in the circuit. Thus, gasification conditions (i.e., high temperature process) must be accurately evaluated, and further studies concerning the technical solutions to achieve a complete conversion in real operating conditions must be performed. It is worth pointing out that even in case of a small accumulation of inert gas in the circuit, there is anyway the possibility of renewing the working fluid by letting a portion of the exhaust gas flow into the air (S7) and making use of auxiliary methane to sustain the process during this transient phase.

It should be noted that the gasification products obtained by Kannan et al. [8] were achieved with a mixture of CO_2 and steam and no nitrogen. The nitrogen content in the present work is considered inert in the gasification process, and the output of the gasifier is computed according to the relative CO_2/steam composition of the gasification agent. The literature seems to be void of results obtained in such condition; therefore, experimental tests in the adopted configuration should be carried out in order to assess the actual composition of the produced synthesis gas.

A greater energy recovery in the exchanger HE6 requires a bigger heat exchanger, thus increasing plant costs. The opportunity to invest in this component can be driven by the usefulness of the cogeneration heat recovered in the exchanger HE7. When the production of process steam or hot air is strongly required, e.g., it may be convenient not to extremize the heat recovery in HE6. These aspects should be taken into consideration in an economic evaluation of the plant, and the best configuration is likely to vary based on the specific industrial destination of use.

It is finally worth noting that in the present activity the electric power required by pumps, fans, and O_2 separator are neglected due to the negligible contribute compared to the total power output, and should be carefully assessed in future studies.

5. Summary and conclusions

In the present study, the thermodynamic feasibility of an innovative closed-loop engine/gasifier power plant was investigated. The main chemical reactions in the CO_2/steam gasifier have been addressed, together with the operating conditions (temperature and CO_2/C ratio) required to correctly run the power plant in closed loop. The power plant components have been described and the results were shown, accounting for two different typologies of destination of use (pure power generation and cogeneration). In detail, accounting for both plastic mix LHV and CH_4 LHV as system input, an efficiency value of 0.154 and 0.443 were respectively obtained in pure power generation and cogeneration configurations, by considering the baseline temperature value of 800 °C at both engine outlet and burner air inlet. Efficiency drastically increases if plastic mix LHV is neglected (i.e., considering plastic as a free source), achieving respectively a value of 1.065 and 3.062 in the two proposed destinations of use. Due to the significance of the two aforementioned temperature values (engine exhaust and burner air inlet) a sensitivity analysis was also shown. It was found that the increase of

these two temperature values leads in both cases to an increase of the power plant efficiency (electrical use) due to the lower CH_4 consumption in the burner and a decrease of the cogeneration efficiency caused by the lower inlet temperature at the heat exchanger dedicated to the thermal user. The effect of the variation of the inlet air temperature at the burner was found to be more pronounced, indicating that it can be considered one of the main tuning parameters of the power plant. In fact, the methane mass flow was found to approach the null value when 900°C are imposed at the burner air inlet, despite precautions must be accounted (in terms of materials) in order to withstand the high thermal stress. Further studies concerning both the technical and economic feasibility must be developed; in particular, technical efforts are required to ensure the complete CO_2 conversion inside the gasifier and a proper evaluation of auxiliary machines is required to better estimate the effective efficiency of the power plant.

Acknowledgments

The Authors would like to sincerely acknowledge Prof. Ing. Ennio Antonio Carnevale for having inspired the present study contributing to the modelling methodology and the conceptualization of the proposed power plant.

References

[1] M.M. Ben Zair, F.M. Jakarni, R. Muniandy, S. Hassim, A.H. Ansari, and Z. Elahi, 2024, Investigation of the fractionalized polyethylene terephthalate (PET) on the properties of stone mastic asphalt (SMA) mixture as aggregate replacement, *Case Stud. Constr. Mater.* 21, doi: 10.1016/j.cscm.2024.e03508.
[2] R. Geyer, J.R. Jambeck, and K.L. Law, 2017, Production, use, and fate of all plastics ever made, *Sci. Adv.* 3(7), doi: 10.1126/sciadv.1700782.
[3] O.O. Ayeleru, S. Dlova, O.J. Akinribide, F. Ntuli, et al., 2020, Challenges of plastic waste generation and management in sub-Saharan Africa: A review *Waste Manag.* 110, doi: 10.1016/j.wasman.2020.04.017.
[4] Q. Qian, J. Ren, and C. He, 2023, Plastic waste upcycling for generation of power and methanol: process simulation and energy–exergy–economic (3E) analysis, *Ind. Eng. Chem. Res.* 62 (43), doi: 10.1021/acs.iecr.3c02665.
[5] L. Bell and P. H. Takada, 2021, Plastic waste management hazards, *International Pollutants Elimination Network (IPEN)*, isbn: 978-1-955400-10-7.
[6] Plastics - the Facts 2022, Plastics Europe AISBL.
[7] G. Lopez, M. Artetxe, M. Amutio, J. Alvarez, J. Bilbao, and M. Olazar, 2018, Recent advances in the gasification of waste plastics. A critical overview, *Renew. Sustain. Energy Rev.* 82, doi: 10.1016/j.rser.2017.09.032.
[8] P. Kannan, G. Lakshmanan, A. Al Shoaibi, and C. Srinivasakannan, 2017, Equilibrium model analysis of waste plastics gasification using CO2 and steam, *Waste Manag. Res.* 35(12), doi: 10.1177/0734242X17736946.
[9] C. Areeprasert, J. Asingsamanunt, S. Srisawat, J. Kaharn, et al., 2017, Municipal plastic waste composition study at transfer station of Bangkok and possibility of its energy recovery by pyrolysis, *Energy Procedia* 107, doi: 10.1016/j.egypro.2016.12.132.
[10] M. Ioelovich, Energy potential of natural, synthetic polymers and waste materials - A review», 2018, *Acad. J. Polym. Sci.* 1(1) 2018, doi: 10.19080/AJOP.2018.01.555553.